Numerical simulation of enhanced heat transfer in heat storage units by metal foam and fins

Zhe Wang[a], Xiaojing Ma[a,b,]*, Shenhua Hu[a], Wei Zhang[a], Jiawen Li[a]

[a]College of Electrical Engineering, Xingjiang University, Urumqi 830047, China;
[b]Engineering Research Center of Northwest Energy Carbon Neutrality, Ministry of Education(ERCNECN), Xinjiang University, Urumqi 830047, China;
*****Corresponding author: Xiaojing Ma; E-mail: maxiaojing1983@xju.edu.cn

Phase change energy storage technology can reduce energy waste, alleviate the energy crisis, and solve the problem of volatility and instability of renewable energy in the utilization process. This paper investigated the enhancement of heat transfer of shell-and-tube heat storage unit by adding tree-shaped fractal fins and metal foam. A three-dimensional numerical model is established, six different heat storage unit tubes are compared to explore the prominent influence of tree-shaped fins and metal foams on the melting process, the thermal performance of varying heat storage unit tubes in the melting process is comprehensively evaluated. The results show that the tree-shaped fractal finned metal foam tubes can significantly enhance the heat transfer to achieve the best heat transfer effect, compared with the smooth tube in terms of the phase change material can be reduced by about 84.7% of the complete melting time; the temperature response rate was increased by 526%, the integral-average heat flux was increased by 376% and the integral-average Nusselt number was increased by 367%.

Keywords: Phase change material; Heat transfer reinforcement; Metal foam; Fins

1. Introduction

As the global demand for energy increases, clean energy is becoming increasingly popular, and solar photovoltaic power generation dominates. Supporting the development of energy storage systems to address its volatility and intermittency is receiving increasing attention. Phase change materials (PCMs) are widely used in solar energy utilization because of their high energy storage density, constant temperature, and good stability, which can compensate for solar energy's inhomogeneity [1]. However, the low thermal conductivity of PCMs significantly affects their energy storage efficiency, so enhancing their heat transfer has always been a research issue. Heat transfer enhancement methods for PCMs mainly include adding fins [2], metal foams [3], nanoparticles [4], and multistage heat transfer enhancement [5].

The fins improve the heat exchange efficiency by increasing the surface area of the heat exchange tube. They can also be designed into different shapes and sizes according to heat exchange requirements to adapt to various working conditions. Due to their simple manufacturing, easy processing, stable performance, and noticeable effect on enhancing heat storage performance, the fins are now widely used to study improved heat transfer in phase change energy storage.

Research has been conducted on the effect of fin size, deflection angle, and number on heat storage

performance. Zhao [6] and Hu et al. [7] investigated the effect of fins with different deflection angles and spacing on the heat storage unit's heat transfer performance. Abhinand S et al. [8] studied the effect of fins added to the heat exchanger tube of a latent heat storage system on the heat transfer process and obtained the optimum number of fins for optimum heat transfer performance. Guo et al. [9] explored the relationship between fin bending angle and heat storage performance of shell and tube heat exchangers by experiment and simulation. Ao et al. [10] designed a series of new three-tube heat exchangers with longitudinal fins to investigate the effect of fins' number, length, thickness, and arrangement on heat storage performance.

In addition to the above studies, some scholars have innovated the fin structure by designing anisotropic fins and investigating their excellent performance in heat transfer. Huang [11], Ren [12], and Roshani et al. [13] designed tree-shaped fins, irregular snowflake-shaped fins, and helical fins to improve the thermal storage performance of the latent heat storage unit, respectively, and it was found that the designed fins improved the thermal storage performance significantly more than the conventional fin structure. Rawat and Sherwan [14] developed a T-shaped fin to simulate the double T-shaped fin melting process in a rectangular, square cavity to obtain the fin length at optimum thermal performance. Hasnain et al. [15] found that using entirely straight, single, and double-branched Y-shaped snowflake fins reduced the PCM melting time more than standard latent heat storage units, with double-branched Y-shaped fins being the most effective.

Most scholars have modified phase change materials to improve heat transfer performance, among them, metal foam has the advantages of high thermal conductivity, high porosity, and large specific surface area. Pu et al. [16] proposed a layered metallic copper foam-filled structure and designed three copper foam gradient types: positive, negative, and uniform non-gradient. The results showed that the negative gradient type has better heat transfer. Wang et al. [17] analyzed the effect of the volume content of copper foam on the melting process of composite phase change material (CPCM). Bouzidi et al. [18] conducted a numerical study on anisotropic layered metallic foams. Meng [19], Iasiello [20], and Wang et al. [21] explored the relationship between the porosity and pore density of the copper foam and the thermal properties of paraffin-metal foam CPCM.

Adding fins or foam metal is a proven way to improve heat storage performance. More studies have been conducted on enhancing phase change heat transfer by single fin and single foam metal. If we combine the high conductivity of solid fin with the uniformly-distributed ability of metal foam, the heat transfer is expected to be further enhanced. Therefore, this paper proposes a tree-shaped fractal finned metal foam heat storage unit tube based on fractal theory. The effect of adding metal foam and fins on heat transfer efficiency was explored. The findings aim to provide higher heat transfer efficiency heat storage units for engineering practice.

2. Geometric model

In 1967, Mandelbrot [22] introduced the concept of fractal to the scientific community, developing fractal theory. The introduction of fractal theory has inspired scholars to think deeply about various phenomena in nature, including the branching distribution of trees, the direction of veins in leaves, and the neural network of the human body. These structures stand out from natural selection and have been proven over time and in practice to show advantages in terms of energy consumption and transmission efficiency. Providing solutions to many optimization problems in engineering, they are therefore applied to phase change thermal storage units.

Fig. 1(b) shows the geometric model of the tree-shaped fractal fin phase change heat storage unit designed. Fig. 1(c) and Fig. 1(d) show the location of the temperature measurement points set up in this paper. A total of nine observation points are set up in the radial and axial directions of the phase change heat storage unit to record the instantaneous temperature to analyze the heat transfer characteristics, with a distance of 15mm between the three points of the same cross-section, and a distance of 75mm between the cross-sections, and at the same time, in order to ensure the uniqueness of the comparison variables, the traditional straight finned tubes and tree-shaped fractal tubes designed have the same fin volume and the same material as the heat exchanger tubes, the diameter of the cylindrical shell is 150mm, the length is 300mm, and the diameter of the inner heat exchanger tube is 30mm with a wall thickness of 1mm, Fig. 2 gives a cross-section of the design of the six groups of cases studied in this paper, In cases A, B and C, paraffin RT35 is used as PCM, and in cases D, E and F, paraffin-foam metal CPCM is embedded in copper foam with a porosity of 0.97 and a pore density of 10PPI to be used as the thermal energy storage medium, water is used as the heat transfer fluid (HTF), and copper is selected as the material for the heat transfer tubes and fins, and the detailed thermo-physical properties of the paraffin RT35 and the copper are shown in Table 1.

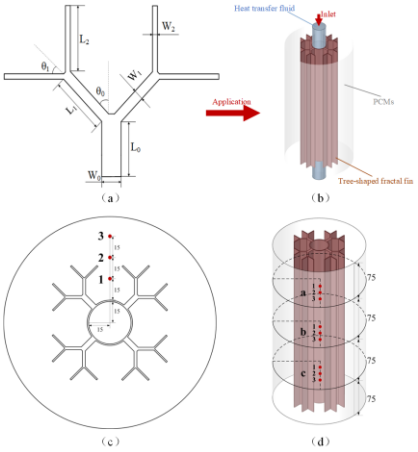

Fig. 1. Tree-shaped fractal fin heat storage unit structure and temperature measurement points：(a)Tree-shaped fractal fin structure; (b)Geometric modeling of a tree-shaped fractal finned heat storage unit tube; (c)Overall measurement points; (d)Cross-sectional measurement points.

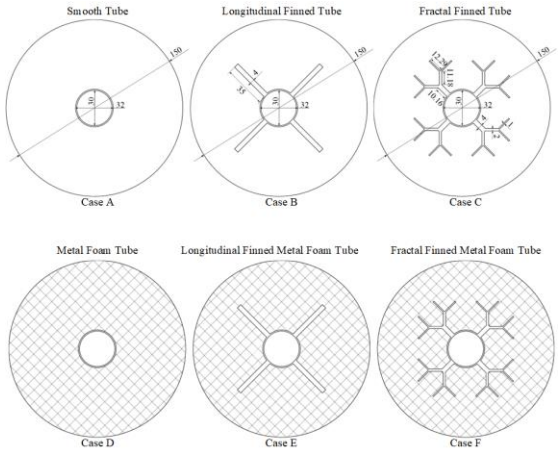

Fig. 2. Cross-section of six types of heat storage unit tubes.

Table 1. Thermo-physical properties of Paraffin RT35 and copper.

Material	Parameter	Value
Paraffin	Melting temperature (°C)	34.7-42.5
	Latent heat ($KJ \cdot Kg^{-1}$)	234.2
	Density ($Kg \cdot m^{-3}$) (solid/liquid)	880/780
	Special heat capacity ($J \cdot Kg^{-1} \cdot K^{-1}$)	2000
	Thermal conductivity ($W \cdot m^{-1} \cdot K^{-1}$) (solid/liquid)	0.2/0.1
	Kinematic viscosity ($m^2 \cdot s^{-1}$)	2.508×10^{-3}

	Thermal expansion coefficient	0.0006
Copper	Density ($Kg\cdot m^{-3}$)	8920
	Special heat capacity ($KJ\cdot Kg^{-1}\cdot K^{-1}$)	380
	Thermal conductivity ($W\cdot m^{-1}\cdot K^{-1}$)	401

3. Numerical simulation

3.1. Governing equations

In this paper, the thermal storage process of PCM is simulated based on the enthalpy-porosity model, and the phase change region is regarded as a porous medium, which is solid when the porosity is zero and liquid when it is 1. A unified energy equation is established in the whole phase change region. The enthalpy distribution is calculated first, and then the solid-liquid phase state is judged according to the enthalpy. The following reasonable assumptions were made to facilitate the analysis: (1) The properties of the solid/liquid phase change material are constant, and the liquid phase change material moves as a laminar, incompressible Newtonian fluid with negligible volumetric thermal expansion. (2) The metallic foam copper is assumed to be homogeneous and isotropic. (3) The Boussinesq approximation is used to solve for the buoyancy effect due to the change in volume of the phase change material, considering natural convection.

The heat transfer process involving metal foam is more complicated than the steady state heat transfer process, in which coupled heat transfer mechanisms such as thermal conductivity of metal foam, thermal conductivity of PCM in different solid and liquid states, and natural convection of liquid PCM are included. To consider the non-Darcy effect of viscous and inertial flow resistance, the Darcy equation promoted by Brinkman-Forchheimer [23] is used in this paper. Additionally, the non-thermal equilibrium equation describes the heat transfer process.

The following controlling equations are used in numerical studies to characterize the flow and heat transfer properties of PCM and metallic copper foam:

$$\frac{\partial \rho_f}{\partial \tau}+\nabla\left(\rho_f \vec{U}\right)=0 \tag{1}$$

$$\frac{\rho_f}{\varepsilon}\frac{\partial u}{\partial \tau}+\frac{\rho_f}{\varepsilon^2}\left(\frac{\partial(uu)}{\partial x}+\frac{\partial(uv)}{\partial y}+\frac{\partial(uw)}{\partial z}\right)=-\frac{\partial p}{\partial x}+\frac{\mu}{\varepsilon}\nabla^2 u-\left(\frac{\mu}{K}+\frac{\rho_f C}{K^{1/2}}\left|\vec{U}\right|\right)u-\frac{(1-\beta)^2}{\beta^3+\delta}A_m u \tag{2}$$

$$\frac{\rho_f}{\varepsilon}\frac{\partial v}{\partial \tau}+\frac{\rho_f}{\varepsilon^2}\left(\frac{\partial(vu)}{\partial x}+\frac{\partial(vv)}{\partial y}+\frac{\partial(vw)}{\partial z}\right)=-\frac{\partial p}{\partial y}+\frac{\mu}{\varepsilon}\nabla^2 v-\left(\frac{\mu}{K}+\frac{\rho_f C}{K^{1/2}}\left|\vec{U}\right|\right)v-\frac{(1-\beta)^2}{\beta^3+\delta}A_m v \tag{3}$$

$$\frac{\rho_f}{\varepsilon}\frac{\partial w}{\partial \tau}+\frac{\rho_f}{\varepsilon^2}\left(\frac{\partial(wu)}{\partial x}+\frac{\partial(wv)}{\partial y}+\frac{\partial(ww)}{\partial z}\right)=-\frac{\partial p}{\partial z}+\frac{\mu}{\varepsilon}\nabla^2 w-\left(\frac{\mu}{K}+\frac{\rho_f C_I}{K^{1/2}}\left|\vec{U}\right|\right)w-\frac{(1-\beta)^2}{\beta^3+\delta}A_m w+\rho g a\left(T_f-T_{m1}\right) \tag{4}$$

$$\varepsilon\rho_f\left(c_f+L\frac{d\beta}{dT_f}\right)\frac{\partial T_f}{\partial \tau}+\rho_f c_f\left(u\frac{\partial T_f}{\partial x}+v\frac{\partial T_f}{\partial y}+w\frac{\partial T_f}{\partial z}\right)=\left(k_{td}+k_{fe}\right)\nabla^2 T_f+h_{sf}a_{sf}\left(T_s-T_f\right) \tag{5}$$

$$(1-\varepsilon)\rho_s c_s\frac{\partial T_s}{\partial \tau}=k_{se}\nabla^2 T_s-h_{sf}a_{sf}\left(T_s-T_f\right) \tag{6}$$

Where ρ_f, c_f, μ, a, L, k_{fe} are the density, specific heat, dynamic viscosity, thermal expansion coefficient, latent heat, and effective thermal conductivity of paraffin wax, respectively, and ε, ρ_s, c_s, k_{se} are the porosity, density, specific heat, and effective thermal conductivity of the metallic copper, respectively. A_m is a parameter of the mushy zone, usually 10^5-10^8, and δ is generally 0.0001 to prevent the denominator from being zero. K and C_I are the permeability and inertial coefficient

for metal foam, T_f and T_s are the temperatures of paraffin and copper metal foam, respectively. The other parameters are derived from semi-empirical formulas in the literature [24-27]. ω, χ, F_I are pore density, flow tortuosity, and inertial force, h_{sf}, a_{sf}, d_p, d_k are interstitial heat transfer coefficient, specific area, pore diameter, and characteristic length, k_{td}, Re_d, Pr are thermal dispersion coefficient, reynolds number, and prandtl number. The numerical calculations determine the liquid phase fraction by the following equation: the solid phase when $\beta = 0$ and the liquid phase when $\beta = 1$. When the paraffin is in the paste region, β is between 0 and 1.

$$\beta = \begin{cases} 0 & T_f \le T_{m1} \\ \left(T_f - T_{m1}\right)/\left(T_{m2} - T_{m1}\right), & T_{m1} < T_f < T_{m2} \\ 1 & T_f \ge T_{m2} \end{cases} \tag{7}$$

T_{m1} and T_{m2} are paraffin melting temperature's lower and upper limits, respectively.

3.2. Boundary and initial conditions

ANSYS-FLUENT 2024 R1 performs numerical simulation, User Define Function (UDF) is used to deal with the interfacial heat transfer coefficients between the metal foam and PCM and the effective thermal conductivity between the two, and the SIMPLE algorithm is used for coupling the pressure field and the velocity field. The momentum and energy equations are discretized using the second-order upwind difference method, and the pressure equations are solved using the PRESTO! algorithm. The continuity, momentum, and energy equation convergence criteria are set to 10^{-5}, 10^{-5}, and 10^{-6}, respectively. The under-relaxation factors for the momentum, pressure, liquid phase fraction, and energy term are set to 0.7, 0.3, 0.9, and 1 to make the calculations converge faster.

In this paper, it is assumed that the initial temperature of HTF and PCM is the same as 22℃, the temperature of HTF is 60℃, the velocity of HTF is 0.2m/s, the exit boundary condition is set as outflow to ensure the conservation of mass, and the coupling boundary condition is used in the interface of the heat transfer tube and HTF as well as the interface of PCM:

$$T_{\mathrm{inner}} = T_{\mathrm{HTF}}, k_{\mathrm{inner}} \frac{\partial T_{\mathrm{inner}}}{\partial n} = k_{\mathrm{HTF}} \frac{\partial T_{\mathrm{HTF}}}{\partial n} \tag{8}$$

$$T_{\mathrm{outer}} = T_{\mathrm{PCM}}, k_{\mathrm{outer}} \frac{\partial T_{\mathrm{outer}}}{\partial n} = k_{\mathrm{PCM}} \frac{\partial T_{\mathrm{PCM}}}{\partial n} \tag{9}$$

All other surfaces are set as adiabatic.

3.3. Validation of numerical simulation

To verify the independence of the model, grid-independence verification and time-step-independence verification are carried out for both longitudinal finned tube and tree-shaped fractal finned tube, and various grid numbers and time steps are selected for testing and comparison. Figure 3 illustrates both tubes' PCM melting fraction profiles at different grid numbers and time steps. In order to save computational resources and improve computational accuracy, 1.2 million grids were selected for the simulation of the tree-shaped fractal finned tube, and 850,000 grids were chosen for the simulation of the regular longitudinal finned tubes in this study. and a time step of 0.5s is chosen for the simulation.

Considering that the UDF program for metal foam effects is compiled as a convective phase change model in ANSYS-FLUENT, this paper validates the transport phenomena in porous media. For the melting of saturated paraffin in open-cell metal foam, Zhang et al. [28] carried out numerical simulation and experimental study on the melting process of paraffin-foam metal composites under

constant heat flux boundaries and set the temperature monitoring points on the metal foam and PCM, respectively. Fig. 4 compares the simulation results in this paper, and Zhang's experiments, numerical simulation of the monitoring points of the temperature curves, and the simulation results in this paper are closer to the literature. The simulation results in this paper are closer to the experimental results than those in the literature. The average relative error is 2.8%, which shows that the established numerical model is reasonable.

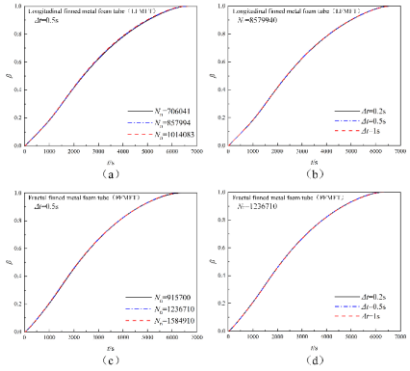

Fig.3. Grid-independent and time-step-independent verification：(a) and (b): LFMFT; (c) and (d): FFMFT.

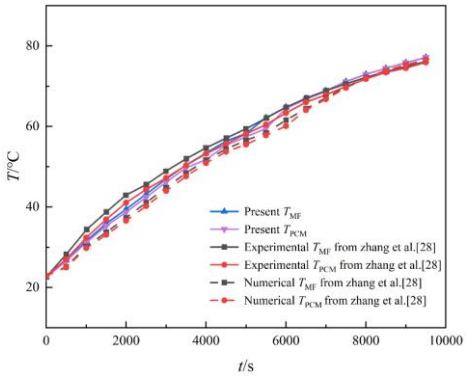

Fig.4. Comparison of numerical simulation results in this paper with numerical simulation results and experimental results in literature 28.

4. Results and discussion

4.1. Liquid phase fraction

To understand the role of fins and metal foam structure in enhancing the phase change heat transfer and storing thermal energy, Fig. 5 compares the variation of PCM melt fraction with time during the melting process of six TES tubes. Fig. 5(a) shows that the presence of fins and metal foam significantly influences the melting process, and there is a considerable difference between their melting times. It can be observed that Fractal Finned Metal Foam Tube (FFMFT) has the fastest melting rate among the six TES tubes, followed by Longitudinal Finned Metal Foam Tube (LFMFT), Metal Foam Tube) MFT, Fractal Finned Tube (FFT), Longitudinal Finned Tube (LFT), and Smooth Tube (ST). In order to better assess the differences between the cases, Fig. 5(b) shows the total melting time of the phase change materials for the six TES tubes. The figure shows that ST has the longest melting time of 40830 s. The melting times of FFMFT, LFMFT, MFT, FFT, and LFT are 6221 s, 6640 s, 9221 s, 10118 s, and 15845 s, respectively. Taking ST as the basis of comparison, the complete melting times of FFMFT, LFMFT, MFT, FFT, and LFT are shortened by 84.7%, 83.7%, 77%, 75% and 61%.

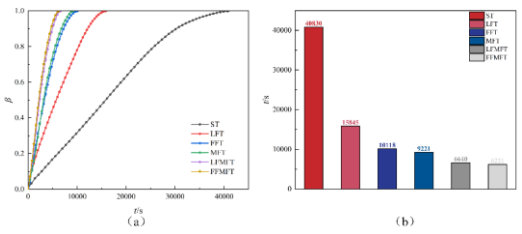

Fig. 5. (a)Liquid phase fraction versus time curves for six types of heat storage unit tubes;(b) Full melting times of PCM for six heat storage unit tubes;

4.2. Evolution and temperature distribution of phase interface

To investigate the solid-liquid phase interface evolution characteristics and temperature distribution of PCM during heat storage, the liquid phase fraction cloud plots and temperature distribution cloud plots of the longitudinal/cross-section of six TES tubes were compared. Fig. 6 shows the liquid phase fraction cloud plots (left half) and temperature distribution cloud plots (right half) of the longitudinal sections of the six TES tubes at 10 min, 50 min, and 90 min. The heat exchanger tube wall is shown in the temperature distribution cloud plots of Fig. 6 to facilitate the differentiation of the temperature regions of the HTF and the paraffin wax. Fig. 7 illustrates the liquid phase fraction cloud (left half) and temperature distribution cloud (right half) at the height H=150 mm cross-section for the six TES tubes at 10 min, 50 min, and 90 min.

For LFT and FFT, it can be observed from the cross-section that the paraffin wax near the fins is the first to melt, the metal fins have high thermal conductivity and heat up rapidly, transferring the temperature to the paraffin wax near the fins, and when the heat storage process is carried out for 90 min, it can be found from the cross-section that the FFT has been completely melted by this time. In contrast, the LFT is only melted by about half. Dramatic differences in the solid-liquid phase interface distribution between the two solutions can also be observed in the longitudinal section. The design of the tree-shaped fractal fins provides a larger contact area through its fractal structure, which helps to increase the contact with the PCM and allows for a more efficient dispersion and transfer of heat, which is more uniformly transferred to the PCM compared to the conventional longitudinal fins and thus accelerates the overall melting process.

For FFMFT, LFMFT, and MFT, the longitudinal and cross-sectional phase interfaces at 10 min were relatively flat and showed a uniform melting trend. The temperature of the paraffin wax close to the tube wall was more homogeneous overall, which was attributed to the fact that the addition of the metal foam reduced the development of buoyancy-induced convection and that the CPCM had much higher thermal conductivity compared to the PCM, resulting in more uniform temperatures in the PCM, The superposition of the fins and the metal foam can increase the melting of the phase change material to strengthen the heat transfer.

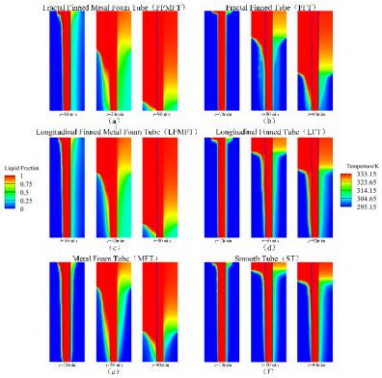

Fig. 6. Schematic of liquid phase fraction and temperature in the longitudinal section at different times for six different heat storage unit tubes:(a) FFMFT; (b) FFT; (c) LFMFT; (d) LFT; (e) MFT; (f) ST.

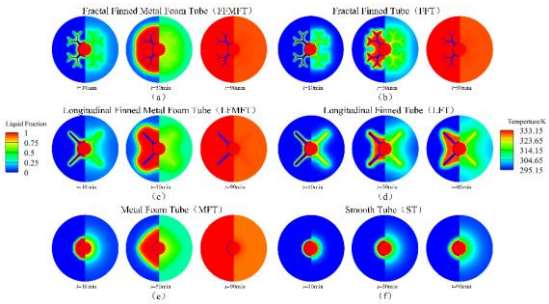

Fig. 7. Schematic of liquid phase fraction and temperature in the cross-section (H=150mm) at different times for six different heat storage unit tubes:(a) FFMFT; (b) FFT; (c) LFMFT; (d) LFT; (e) MFT; (f) ST.

4.3. Temperature response

To investigate the temperature change of the PCM during the melting process in different cases, this paper selected three layers of distinct heights of the phase change material plane in the axial direction to take points and three different points in the radial direction of the same height to carry out temperature measurements, the distance between the points is 15mm, and the measurement point near the wall is 15mm away from the exterior wall of the HTF. The heights of the three layers of the plane were selected as follows: 75mm (measurement points of this layer are a_1, a_2, a_3), 150mm (measurement points of this layer are b_1, b_2, b_3), and 225mm (measurement points of this layer are c_1, c_2, c_3) as shown in Fig. 1.

As can be obtained from the radial temperature profiles in Fig.8, closer proximity to the thermal boundary wall will initially cause the PCM to rise faster, creating a temperature gradient in the radial direction. In addition, the temperature difference between the three points will gradually decrease in the later stages of thermal storage, mainly since the PCM will change from a solid to a liquid over time, and natural convection will occur when the solid-liquid interface is submerged in the horizontal plane of these three selected points. As a result, the temperature gradient of the paraffin wax decreases in the radial direction. It can be observed that the temperature variation curve of the heat storage tube with metal foam in the figure is the most concentrated, indicating that the metal foam can effectively improve the temperature field uniformity in the PCM domain.

The axial temperature profiles in Fig. 9 demonstrate a slight temperature difference between the three selected points, with nearly overlapping profiles during the early heat storage stage. This is mainly due to the vast temperature difference between the HTF and the solid PCM near the HTT tube wall, which provides a high heat flux for the melting of the PCM in this region. In addition, natural convection did not form steadily at an early stage, and the effect of localized natural convection in the PCM on the early melting stage can be neglected. The time to reach the steady temperature was much longer for ST than for the other five TES tubes because the thermal conductivity of the phase change material was too low to transfer enough heat energy farther away from the copper tube wall. Adding enhanced heat transfer devices through fins and metal foams and their combinations causes heat to spread rapidly, increasing temperature differences along the HTF flow direction. Over time, more PCM melts into liquid, providing more room for natural convection.

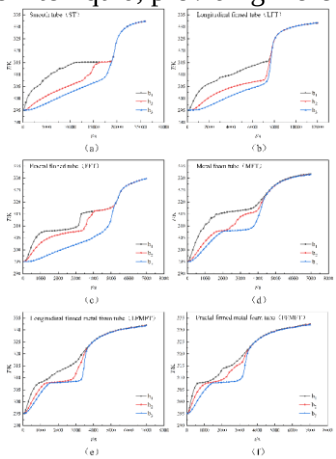

Fig. 8. Temperature profiles of selected radial points of six different heat storage unit tubes:

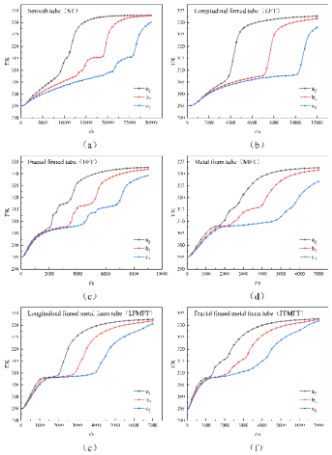

Fig. 9. Temperature profiles of selected axial points of six different heat storage unit tubes:

(a) ST; (b) LFT; (c) FFT; (d) MFT; (e) LFMFT; (f) FFMFT.

(a) ST; (b) LFT; (c) FFT; (d) MFT; (e) LFMFT; (f) FFMFT.

In order to quantitatively investigate the effect of the six heat storage tubes on the radial temperature response of the PCM, the integral-averaged temperature response rate $\overline{RR}$ is used to quantitatively describe it, which is expressed as:

$$\overline{RR}=\int_0^{t_{\text{full}}}\frac{1}{t_{\text{full}}}\frac{T(t_i)-T(t_{i-1})}{(t_i-t_{i-1})}\mathrm{d}t \tag{10}$$

Where and $T(t_{i-1})$ are the temperatures at t_i and t_{i-1}, and t_{full} denotes the complete melting time for each case. Fig. 10(a) illustrates the temperature profile during the melting process at point b_2 for six different TES tubes. From the figure, it can be seen that FFMFT achieves the fastest warming, the temperature gradient changes of FFMFT and LFMFT are not much different in general, and FFMFT warms up slightly faster than LFMFT, followed by MFT, FFT, LFT, and ST. During the heat storage process, the heat conducted by the fins will be effectively absorbed by the PCM near the fins, and the metal foam uniformly and rapidly transfers the heat to the PCM further away through its rich specific surface area and high thermal conductivity, which further enhances the heat transfer and achieves more rapid warming. Fig. 10(b) demonstrates the integral-average temperature response rate of the six TES tubes at point b_2. It can be observed that FFMFT has the largest integral-average temperature response rate, followed by LFMFT, MFT, FFT, LFT, and ST. Adding fins and metal foam increases the integral-average temperature response rate, and the enhancement effect of fins and metal foam together is more obvious. Taking ST as the basis of comparison, the integral-average temperature response rate of LFT, FFT, MFT, LFMFT, and FFMFT are increased by 155%, 296%, 334.7%, 488%, and 526%, respectively.

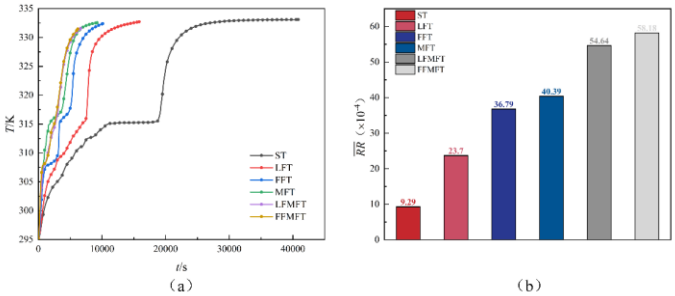

Fig. 10. Temperature response of six different heat storage unit tubes: (a) Temperature variation curves at selected point b2; (b) Histogram of the integral-averaged temperature response rate during PCM melting process.

4.4. Heat exchange rate

The phase interface evolution process and temperature response distribution were shown above, and to more fully compare the heat exchange performance of the six different heat storage tubes, the integral-average heat flux is used below to analyze the heat exchange rate of the heat storage process of other cases of PCM. The integral-average heat flux of the whole heat storage process can be calculated based on the following equation:

$$\bar{q}=\frac{\int_0^{t_{\text{full}}}q_{\text{w}}(t)\mathrm{d}t}{t_{\text{full}}} \tag{11}$$

$\bar{q}$ is the integral-averaged heat flux over the entire melting time, and q_{w} is the heat flux at the

inner surface of the HTF tube. Fig 11(a) shows the integral-averaged heat fluxes of the six TES tube phase change materials during the melting process. It can be seen that FFMFT has the largest integral-average heat flux and the fastest heat transfer rate, followed by LFMFT, MFT, FFT, LFT, and ST. Taking the integral-average heat flux of ST as a benchmark, the integral-average heat flux of LFT during the heat storage process increased by 136.6%, that of FFT increased by 233%, that of MFT increased by 233.2%, that of LFMFT increased by 335%, and FFMFT increased by 376%. Adding fins and metal foam can increase the heat exchange rate; the difference in the integral-average heat flux between the tree-shaped fractal fins and metal foam tubes is not much; adding metal foam to finned tubes can significantly increase heat exchange rates.

The integral-average Nusselt number is used to describe the average heat transfer effect over the entire heat transfer surface. It is used here to compare the heat transfer capacity in the six TES tubes throughout the melting process, and it is expressed as:

$$\overline{Nu} = \int_0^{t_{\text{full}}} \frac{q_{\text{w}}(t) D}{(T_{\text{HTF}} - T_{\text{w}}) k_f t_{\text{full}}} \mathrm{d}t \tag{12}$$

Where q_{w} is the heat flux at the inner surface of the HTF tube, t_{full} is the complete melting time, D is the diameter of the tube, k_f is the thermal conductivity of liquid PCM, and T_{HTF} and T_{w} are the temperatures of the HTF and the inner surface of the HTF tube. From Fig. 11(b), the FFMFT has the largest integral-average Nusselt number of 151.12 in the heat storage process, followed by the LFMFT, MFT, FFT, LFT, and ST, whose integral-average Nusselt numbers are 143.69, 107.72, 96.61, 69.92, and 32.34, respectively. Taking the integral-average Nusselt number of ST as a benchmark, the LFT increased by 116%, the FFT by 198.7%, and the MFT by 233% during the heat storage process. the LFMFT increased by 344%, and the FFMFT increased by 367%.

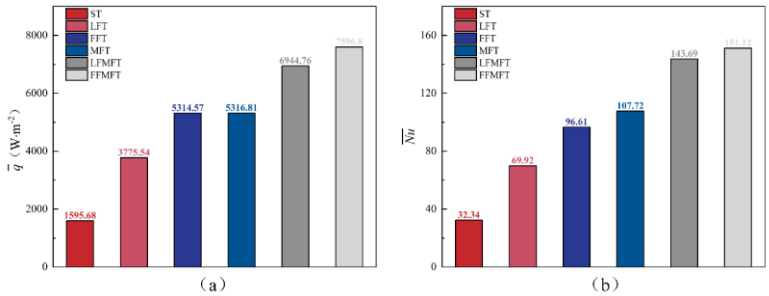

Fig. 11. The integral-average heat flux and the integral-average Nusselt number of six different heat storage unit tubes during PCM melting process.

5. Conclusion

In this paper, the melting process of paraffin wax in six different types of phase change heat storage unit tubes is numerically investigated. By comparing the total melting time, solid-liquid phase interface, temperature response, and heat exchange rate, the heat transfer enhancement effect of fins and metal foams on the shell-and-tube phase change heat storage unit is investigated, and the following conclusions are drawn:

Tree-shaped fractal finned metal foam tube can significantly enhance heat transfer to achieve the best heat transfer effect. Compared with the smooth tube, the phase change material can be reduced by about 84.7% of the complete melting time; the integral-average temperature response rate increased by 526%; the integral-average heat flux increased by 376%, and the integral-average Nusselt number increased by 367%.

Comparing the temperature profiles at the measurement points of the six types of heat storage unit tubes, it is found that the temperature change profiles of the tubes with metal foam are more centralized, and the axial and radial temperature gradients are smaller, indicating that the metal foam effectively improves the uniformity of the temperature field of the phase change material.

In the absence of metal foam within the heat storage unit tube, the fin structure plays a crucial role in enhancing overall heat storage performance. It effectively reduces melting time and improves both the temperature response and heat transfer rate. When metal foam is present, the fin structure continues to influence thermal performance, albeit to a lesser extent.

Acknowledgment

This work was supported by National Natural Science Foundation of China (12362021), Xinjiang Uygur Autonomous Region Tianshan Talent Training Program-Youth Talent Support Project (2022TSYCCX0054), Key Research and Development Task Special Project of Xinjiang Uygur Autonomous Region (2022B03028-5), and Hami Hi-Tech Industrial Development Zone Scientific Research and Technology Development Program (HGX2024KJXM007).

References

[1] Jayathunga, D. S., et al., Phase change material (PCM) candidates for latent heat thermal energy storage (LHTES) in concentrated solar power (CSP) based thermal applications-a review. *Renewable and Sustainable Energy Reviews*, 189(2024), pp. 113904

[2] Lee, Y. T., et al., Numerical and experimental investigations on melting heat transfer performance of PCM in finned cold thermal energy storage. *International Journal of Heat and Mass Transfer*, 210(2023), pp. 124199.

[3] Xiao, T., et al. Melting of phase change materials inside metal foams with uniform/graded porosity: Pore-scale simulation. *Applied Thermal Engineering*, 232(2023), pp. 121082.

[4] Bharathiraja, R., et al., Thermal characteristics enhancement of Paraffin Wax Phase Change Material (PCM) for thermal storage applications. *Renewable Energy*, 222(2024), pp. 119986.

[5] Yin, L., et al., Flow boiling heat transfer in multi-stage enhanced open microchannels with micro/nano structures. *Applied Thermal Engineering*, 258(2025), pp. 124695.

[6] Zhao, C., et al., Fin design optimization to enhance PCM melting rate inside a rectangular enclosure. *Applied Energy*, 321(2022), pp. 119368.

[7] Hu, Z., et al., Numerical simulation of fin arrangements on the melting process of PCM in a rectangular unit. *Renewable Energy*, 220(2024), pp. 119677.

[8] Abhinand, S., et al., Performance analysis of PCM melting in a fin-assisted thermal energy storage system–a numerical study. *International Communications in Heat and Mass Transfer*, 144(2023), pp. 106747.

[9] Guo, J., et al., Melting assessment on the angled fin design for a novel latent heat thermal energy storage tube. *Renewable Energy*, 183(2022), pp. 406-422.

[10] Ao, C., et al., Assessment on the effect of longitudinal fins upon melting process in a latent heat thermal energy storage unit. *Journal of Energy Storage*, 59(2023), pp. 106408.

[11] Huang, Y., and Liu, X. Charging and discharging enhancement of a vertical latent heat storage unit by fractal tree-shaped fins. *Renewable Energy*, 174(2021), pp. 199-217.

[12] Ren, F., et al., Optimization on a novel irregular snowflake fin for thermal energy storage using response surface method. *International Journal of Heat and Mass Transfer*, 200(2023), pp. 123521.
[13] Roshani, M., et al., Enhancing geothermal heat pump efficiency with fin creation and microencapsulated PCM: A numerical study. *Journal of Energy Storage*, 95(2024), pp. 112664.
[14] Rawat, P., and Sherwani, A. F A, numerical study on the impact of fin length arrangement and material on the melting of PCM in a rectangular enclosure. *International Journal of Heat and Mass Transfer*, 205(2023), pp. 123932.
[15] ul Hasnain, F., et al., Melting performance enhancement of a phase change material using branched fins and nanoparticles for energy storage applications. *Journal of Energy Storage*, 38(2021), pp. 102513.
[16] Pu, L., et al., Numerical study on the performance of shell-and-tube thermal energy storage using multiple PCMs and gradient copper foam. *Renewable Energy*, 174(2021), pp. 573-589.
[17] Wang, Z., et al., Effect of copper metal foam proportion on heat transfer enhancement in the melting process of phase change materials. *Applied Thermal Engineering*, 201(2022), pp. 117778.
[18] Bouzidi, M., et al., Charging and discharging heat transfer improvement of shell-tube storage utilizing a partial layer of anisotropic metal foam. *Journal of Energy Storage*, 79(2024), pp. 109948.
[19] Meng, X., et al., Effect of porosity and pore density of copper foam on thermal performance of the paraffin-copper foam composite Phase-Change Material. *Case Studies in Thermal Engineering*, 22(2020), pp. 100742.
[20] Iasiello, M., et al., Metal foam/PCM melting evolution analysis: Orientation and morphology effects. *Applied Thermal Engineering*, 187(2021), pp. 116572.
[21] Wang, Z., et al., Effect of enhancement in metal foam pore density on heat transfer of phase-change materials. *International Communications in Heat and Mass Transfer*, 144(2023), pp. 106750.
[22] Mandelbrot, B. B., et al., Fractal character of fracture surfaces of metals. *Nature*, 308(5961) (1984), pp. 721-722.
[23] Cui, H. T. Experimental investigation on the heat charging process by paraffin filled with high porosity copper foam. *Applied thermal engineering*, 39(2012), pp. 26-28.
[24] Xu, Y., et al., Evaluation and optimization of melting performance for a latent heat thermal energy storage unit partially filled with porous media. *Applied energy*, 193(2017), pp. 84-95.
[25] Mahdi, J. M., et al., Intensifying the thermal response of PCM via fin-assisted foam strips in the shell-and-tube heat storage system. *Journal of Energy Storage*, 45(2022), pp. 103733.
[26] Georgiadis, J. G., and Catton, I., Dispersion in cellular thermal convection in porous layers. *International journal of heat and mass transfer*, 31(5) (1988), pp. 1081-1091.
[27] Yang, X., et al., Solidification in a shell-and-tube thermal energy storage unit filled with longitude fins and metal foam: A numerical study. *Energy and Built Environment*, 4(1) (2023), pp. 64-73.
[28] Zhang, P., et al., Melting heat transfer characteristics of a composite phase change material fabricated by paraffin and metal foam. *Applied Energy*, 185 (2017), pp. 1971-1983.

Submitted 24.05.2025
Revised: 01.08.2025
Accepted: 28.08.2025